JOURNAL OF CATALYSIS 144, 425–438 (1993)

Influence of the Preparation Methods of V–Mg–O Catalysts on Their Catalytic Properties for the Oxidative Dehydrogenation of Propane

A. CORMA, J. M. LÓPEZ NIETO,[1] AND N. PAREDES

Instituto de Tecnología Química, UPV-CSIC, c/Camino de Vera s/n, 46071 Valencia, Spain

Received March 2, 1993; revised June 2, 1993

The influence of the preparation methods of V–Mg–O catalysts on their catalytic properties in the oxidative dehydrogenation of propane has been studied. By using MgO with surface areas from 49 to 141 $m^2 g^{-1}$ as supports, and carrying out the incorporation of vanadium starting from vanadyl oxalate or ammonium metavanadate, it has been found that different V species are formed, with V/Mg ratios at the catalyst surface ranging from 0.02 to 0.5. A new preparation procedure which allows a homogeneous dispersion of vanadium along the MgO is presented. The highest activity and selectivity are obtained on catalysts with an Mg-enriched surface in which isolated VO_4 tetrahedra are present. Similar trends for the influence of the V/Mg surface atomic ratio on the selectivity to propene and for the shift of the binding energy (B.E.) of the O1*s* line, obtained by XPS, are observed. The higher the shift of the B.E. of the O1*s* line, the higher the selectivity to propene. For this reason, a correlation between the low nucleophilic character of the oxygen and the selectivity for the ODH of alkanes has been tentatively proposed.

INTRODUCTION

V–Mg–O catalysts are active and selective in the oxidative dehydrogenation (ODH) of propane (*1–3*). Also, these catalysts are effective in the ODH of *n*-butane (*1, 4*), 1-butene (*5, 6*), cyclohexane (*7*), or ethyl-benzene (*5, 8*). In addition, other metallic orthovanadates have been proposed as effective catalysts in the ODH of alkanes but high selectivities to olefins are only obtained at low alkane conversion levels (*9–12*).

The presence of isolate VO_4 tetrahedron, as well as the absence of V=O double bonds, and differences in the redox properties of the cations in metallic vanadates (*4, 10–14*) have been proposed as responsible for the oxydehydrogenation properties of vanadium-based catalysts.

In the case of V–Mg–O catalysts, the presence of $Mg_3V_2O_8$ (*1, 2*) and/or α-$Mg_2V_2O_7$ (*3*), result in catalysts with high activity and selectivity for the ODH of propane. However, only catalysts containing isolated VO_4 tetrahedra at the catalyst surface (*16*) or the $Mg_3V_2O_8$ phase (*11, 15, 17*) show better selectivity in the ODH of *n*-butane.

The obtenation of a determinated Mg-vanadate phase ($Mg_3V_2O_8$, α- and β-$Mg_2V_2O_7$ or MgV_2O_6) is controlled by the preparation procedure. Then, starting from a V_2O_5/MgO molar ratio of 1 : 3, the Mg-orthovanadate is formed only at long calcination times, while the Mg-pyrovanadate is the principal phase at intermediate calcination times (*18*). In catalysts prepared by impregnation methods, and with low vanadium contents, Mg-orthovanadate and MgO are obtained. However, if potassium impurities are present (*15*) or an Mg-silicate is used as support (*13, 14*), Mg-vanadates other that $Mg_3V_2O_8$ are formed, concluding that the formation of $Mg_3V_2O_8$ can be suppressed or slowed down due to the presence of different impurities.

In the present paper, V–Mg–O catalysts have been prepared using different preparation procedures which involve modifica-

[1] To whom correspondence should be addressed.

0021-9517/93 $5.00

tions in: the source of V, the characteristics of MgO, and the incorporation of V on the MgO. The different phases formed have been characterized, and the influence of the preparation methods on their catalytic properties in the ODH of propane is presented.

EXPERIMENTAL

Catalyst Preparation

V–Mg–O catalysts were prepared by impregnation, using as support three magnesium oxides and a magnesium oxalate. The preparation of the supports was carried out according to the following methods:

(a) By precipitation, at pH $\approx$ 5–6, of a magnesium acetate solution with an oxalic acid solution. The solid obtained was filtered, washed, and dried at 80°C for 16 h (*19*). This solid was identified as magnesium oxalate, β-MgC_2O_4 (Mg*X*). The calcination of Mg*X* at 700°C for 3 h produces a magnesium oxide denoted MgO-1.

(b) By precipitation, at pH 10, of an Mg-sulphate solution with an NH_4OH solution. In these conditions $Mg(OH)_2$ was obtained (*20*), and after filtering, washing, and drying at 80°C for 16 h, it was calcined at 600°C for 6 h to produce a magnesium oxide denoted MgO-2.

(c) By precipitation, at pH 6.5, of a magnesium nitrate solution with an $(NH_4)_2CO_3$ solution (*1*). After filtering, washing, drying at 80°C for 16 h, and calcining at 700°C for 3 h, a magnesium oxide denoted MgO-3 was obtained.

Vanadium supported catalyst were prepared using ammonium metavanadate (AV) or vanadyl oxalate (VO) solutions as vanadium precursors.

MgO-1 and MgO-3 samples were impregnated with an AV solution, using the procedure described previously (*1*). Then, it was dried at 70°C, kept at 80°C for 16 h, and, finally, calcined in air at 550°C for 3 h. The resulting catalysts were denoted V/MgO-1 or V/MgO-2 series.

MgO-2 or Mg*X* were impregnated with a VO-solution (containing a V_2O_5/oxalic acid molar ratio of 1/3), dried in a rotavapor at 90°C, then kept at 80°C for 16 h, and finally calcined in air at 550°C for 3 h. The resulting catalysts were denoted VO/MgO-2 or VO/Mg*X*.

The vanadium magnesium catalysts referred to as V/MgO-1, V/MgO-3, VO/MgO-2, and VO/Mg*X* are preceded by a number that indicates the wt% of vanadium given as V_2O_5.

Catalyst Characterization

The specific surface area of the catalysts and supports were obtained by using the BET method, from the nitrogen isotherms at 77 K in an ASAP 2000 apparatus, and taken 0.164 nm^2 as the cross-section of nitrogen.

X-ray diffraction (XRD) patterns were obtained using a Phillips 1060 diffractometer operated at 40 kV and 20 mA employing nickel-filtered Cu$K\alpha$ radiation (λ = 0.1542 nm).

The infrared spectra were recorded at room temperature in a Nicolet 205xB spectrophotometer equipped with a Date station.

The laser Raman spectra were recorded with a Dilor spectrometer. The emission line at 484 and 514.5 nm from Ar^+ (spectra Physics, Model 165) was used for excitation. The output power of the laser was reduced to 25 mW to avoid sample volatilization. The sensitivity was adjusted according to the intensity of Raman scattering. Wavenumbers reported in the spectra are accurate within $\sim$2 cm^{-1}.

Thermogravimetric analysis were performed on a Nestz system over the temperature range 30–800°C. The reference material was Al_2O_3 previously ignited at 1100°C. The sample and reference were located in platinum crucibles. The measurements have been carried out at a heating rate of 10°C/min, under a flow of air (100 ml/min).

X-ray photoelectron spectroscopy (XPS) data were obtained in a Leybold Heraeus LHS 10 spectrometer, working in the ΔE = constant mode, interfaced to a data system which allowed accumulation of spectra. The

spectrometer was equipped with a magnesium anode (Mg$K\alpha$ = 1253.6 eV), operated at 12 kV and 10 mA. The samples were outgassed at room temperature to a pressure of 10^{-9} Torr. A binding energy (B.E.) of 83.8 eV, corresponding to the Au/$4f_{7/2}$ peak, was used as an internal reference. The accuracy of the B.E. as determined with respect to this standard value was within ±0.2 eV. Ratios of the atomic concentrations in the outer surface layers of the samples were estimated from the corresponding XPS peak area ratios using the equation

$$(V/Mg)_{XPS} = (\Delta_V/\Delta_{Mg})(\sigma_{Mg}/\sigma_V)(\lambda_{Mg}/\lambda_V)(KE_V/KE_{Mg})^{1/2}$$

where σ is the effective ionization cross-section of ejected electrons calculated and tabulated by Scofield (*21*), KE is the kinetic energy of the electrons, Δ is the normalized peak area after linear background subtraction, and λ is the escape depth which was calculated from the formulas given by Vullis and Starke (*22*).

Catalytic Experiments

The catalytic experiments were carried out in a fixed bed, continuous stainless steel tubular reactor (i.d. 20 mm; length 520 mm). A coaxially centered thermocouple was used, which could be moved up and down along the catalyst bed for temperature profiling. The catalyst charge was 0.5–1.0 g (particle size 0.25–0.42 mm) mixed with Norton Silicon Carbide (particle size 0.59 mm) to obtain a total volume of 3 cm^3. All experiments were conducted at atmospheric pressure. The feed consisted of propane, oxygen and helium in a molar ratio of 4/8/88. Different contact times, W/F in a g_{cat} h (mol $C_3H_8)^{-1}$, were used to obtain different propane conversion levels. The reaction has been studied in the temperature interval 400–550°C.

Blank runs showed that under the experimental conditions used in this work the homogeneous reaction can be neglected. In all cases, the lower flow used was 100 ml min^{-1}.

Analysis of reactants and products were carried out by gas chromatography using three columns: (i) plot capillary, 50 m; (ii) Molecular Sieves 5A (1.5 m × $\frac{1}{8}$″); (iii) porapak Q (3.0 m × $\frac{1}{8}$″).

TABLE 1

Magnesium Oxides Used as Support

Support[a]	Precursor	S_{BET} (m^2/g)	V pore (cm^3/g)
MgO-1	Magnesium oxalate	141	16.8
MgO-2	Magnesium sulphate	95.2	0.65
MgO-3	Magnesium nitrate	49.3	—

[a] MgO with different surface area.

RESULTS

Catalyst Characterization

The specific surface area of the support, as well as, the chemical composition and the specific surface area of the catalysts are presented in Tables 1 and 2, respectively. Large differences in the specific surface area of MgO were obtained depending on the preparation procedure. In addition, sensible differences in the specific surface areas of V–Mg–O catalysts were observed, depending on the preparation method, support, and vanadium content. In the VO/MgX series the higher the vanadium content the lower the specific surface area was.

The DTA curves obtained for different catalysts are shown in Fig. 1. For comparison, the DTA curve obtained from a magnesium oxalate, MgX, is also included (Fig. 1a). In this sample an endothermic peak at ~205°C, due to the elimination of crystallization water, and an exothermic peak at ~490°C associated to the degradation of organic compounds is observed. Meanwhile, in VO/ MgX other peaks besides the two observed in the MgX sample are obtained: (i) an endothermic peak at 150–170°C that can be assigned to elimination of water interacting with the vanadyl oxalate; (ii) an exothermic peak at 250–300°C, corresponding to the degradation of organic compounds interacting with vanadium; and (iii) an exothermic peak at ~410°C, which is only ob-

TABLE 2

Physicochemical Characteristics of V–Mg–O Catalysts

Sample	S_{BET}	V_2O_5 (wt%)	$(V/Mg)_{CA}$ atomic ratio[a]	Method
7VO/Mg*X*	141.9	7.1	0.034	Vanadyl oxalate on magnesium oxalate
20VO/Mg*X*	136.0	19.7	0.109	Vanadyl oxalate on magnesium oxalate
34VO/Mg*X*	101.6	33.5	0.224	Vanadyl oxalate on magnesium oxalate
48VO/Mg*X*	42.8	48.1	0.412	Vanadyl oxalate on magnesium oxalate
18VO/MgO-2	88.83	18.3	0.099	Vanadyl oxalate on MgO-2
38VO/MgO-2	87.94	37.5	0.266	Vanadyl oxalate on MgO-2
19V/MgO-1	118.1	19.3	0.106	Ammonium metavanadate on MgO-1
19V/MgO-3	59.9	19.0	0.104	Ammonium metavanadate on MgO-3

[a] V/Mg atomic ratio was done by atomic absorption spectrometry.

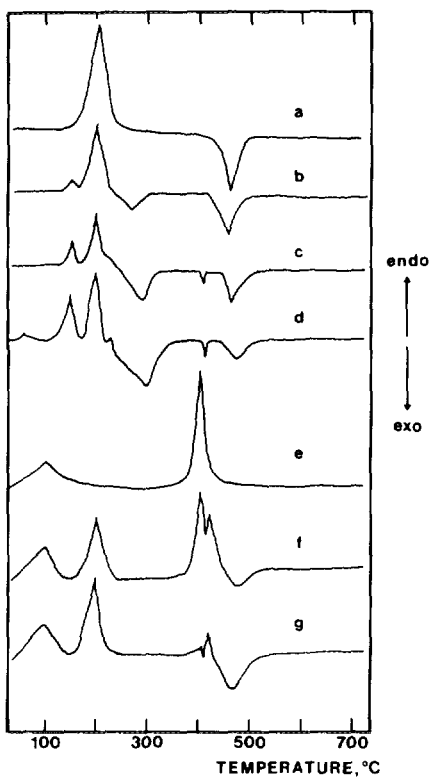

FIG. 1. DTA curves of V–Mg–O catalysts: (a) magnesium oxalate, (b) 20VO/Mg*X*, (c) 34VO/Mg*X*, (d) 48VO/Mg*X*, (e) 19V/MgO-1, (f) 18VO/MgO-2, and (g) 38VO/MgO-2. Composition and preparation methods in Table 2.

served on 34VO/Mg*X* (Fig. 1c) and 47VO/Mg*X* (Fig. 1d) samples and which corresponds to the formation of α-$Mg_2V_2O_7$ (*3*).

Some differences in the DTA curves of MgO-impregnated samples were observed, specially in the range 400–500°C. In the V/MgO series (Fig. 1e), the presence of an endothermic peak at 400°C could be assigned to the formation of MgO from the decomposition of $Mg(OH)_2$, in accordance with our XRD results of the non calcined samples (*23*) and the DTA data obtained from the $V_2O_5/Mg(OH)_2$ samples (*3*).

In the case of the VO/MgO-2 series, the decomposition of $Mg(OH)_2$ (endothermic peak at 400°C) is observed in the 18VO/MgO-2 (Fig. 1f) but it is not clearly seen in the 38VO/MgO-2 sample (Fig. 1g). In addition to this, the exothermic peak at ~470°C (corresponding to decomposition of Mg-oxalate) is observed in the two samples, although this peak is more intense in the 38VO/MgO-2 sample. We must indicate that α-$Mg_2V_2O_7$ (exothermic peak at 410°C) and $Mg_3V_2O_8$ (endothermic peak at 420°C) are also observed even though the corresponding intensities are low.

XRD of the calcined samples are shown in Figs. 2 and 3. The presence of MgO and $Mg_3V_2O_8$ is observed in all catalysts, except in the 7VO/Mg*X* and 18VO/MgO-2 samples in which only MgO was observed. On the

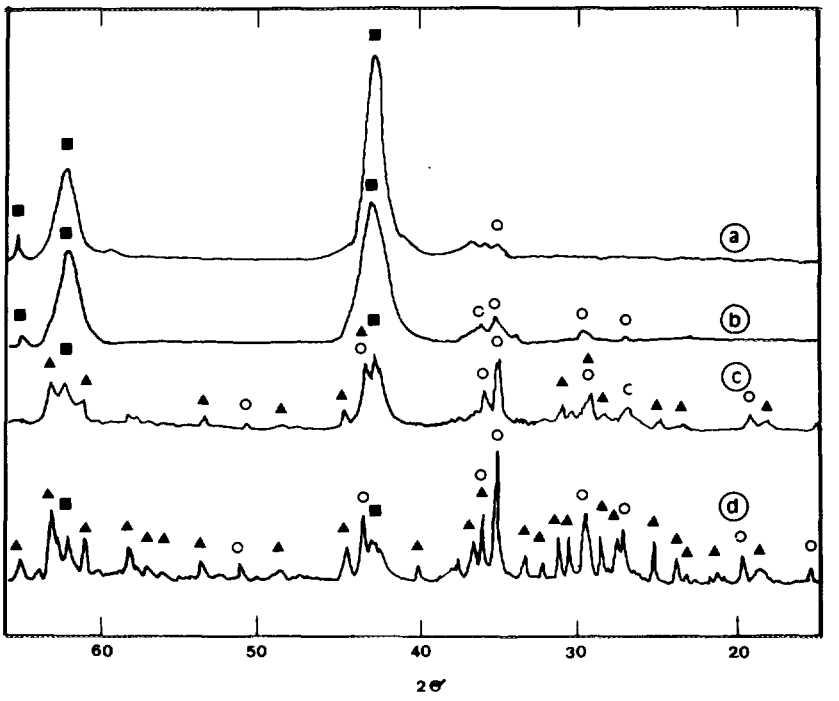

FIG. 2. XRD patterns of the VO/MgX catalysts with different vanadium content: (a) 7VO/MgX, (b) 20VO/MgX, (c) 34VO/MgX, and (d) 48VO/MgX. Symbols: (■) MgO, (○) $Mg_3V_2O_8$, and (▲) α-$Mg_2V_2O_7$.

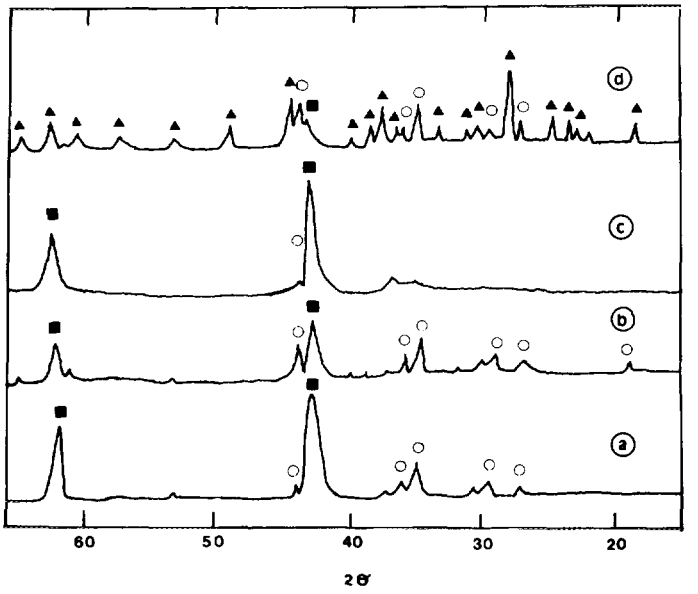

FIG. 3. XRD patterns of catalysts prepared by impregnation of MgO: (a) 19V/MgO-3, (b) 19V/MgO-1, (c) 18VO/MgO-2, and (d) 38VO/MgO-2. Symbols as Fig. 1.

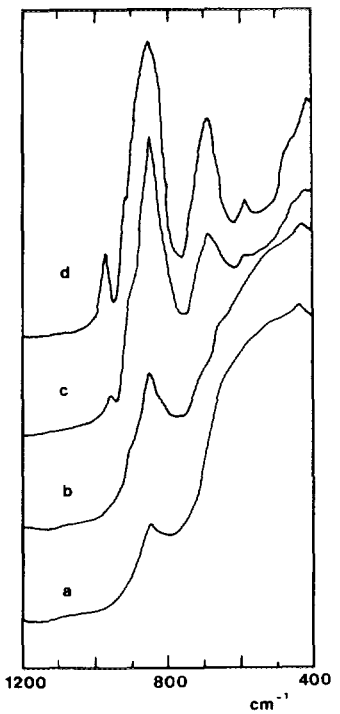

FIG. 4. Infrared spectra of the VO/MgX series: (a) 7VO/MgX, (b) 20VO/MgX, (c) 34VO/MgX, and (d) 48VO/MgX.

other hand, in catalysts with high vanadium loading (>25 wt%), α-$Mg_2V_2O_7$, in addition to MgO and $Mg_3V_2O_8$, has been observed.

In the infrared spectra (Figs. 4 and 5) the presence of bands at 916, 860 and 690 cm^{-1} are observed in all catalysts, including the 7VO/MgX and 18V/MgO-2 samples. These bands can be associated to the presence of $Mg_3V_2O_8$ (*3, 4, 8*). In samples with high vanadium content, the presence of bands at 968 and 575 cm^{-1}, in addition to the bands at 916, 860, and 690 cm^{-1}, indicate the presence of α-$Mg_2V_2O_7$ and $Mg_3V_2O_8$ (*3, 4, 8*).

Similar conclusion can be reached from the Raman spectra of the 7VO/MgX and 18VO/MgO-2 samples (Figs. 6a and 6b, respectively) in which the presence of bands at 850 and 820 cm^{-1} clearly show the presence of $Mg_3V_2O_8$ (*8, 14, 24*). Moreover, the bands at 940 and 902 cm^{-1} observed in samples with high vanadium content (Figs. 6c and 6d), can be assigned to an α-$Mg_2V_2O_7$ phase (*8, 14, 24*). We must indicate that in catalysts containing ≤20 wt% of V_2O_5, the broad band centered at 860 cm^{-1} in Raman spectra could indicate the presence of smaller amounts of other magnesium-vanadates (α-$Mg_2V_2O_7$ or β-$Mg_2V_2O_7$) and isolated VO_4 tetrahedra. Thus, by Raman spectroscopy those has been observed in the 950–900 cm^{-1} range while isolated VO_4 tetrahedra has been observed at 800 cm^{-1} (*14*).

The surface composition of the catalysts was determined by XPS measurements. The binding energies (B.E.) obtained for the C1s, O1s, Mg2p, and V2$p_{3/2}$ lines are presented in Table 3. For the C1s lines two values, corresponding to carbon on the surface (B.E. = 284.9 eV) and C=O bonds (B.E. ~289.5 eV), are obtained. While a similar value for the V2$p_{3/2}$ line (B.E. ~517.1 ± 0.2 eV) was observed on the different catalysts, small differences in the

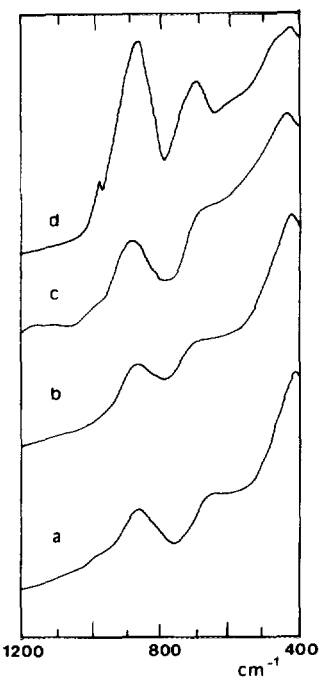

FIG. 5. Infrared spectra of catalysts prepared by impregnation of MgO: (a) 19V/MgO-1, (b) 19V/MgO-3, (c) 18VO/MgO-2, and (d) 38VO/MgO-2.

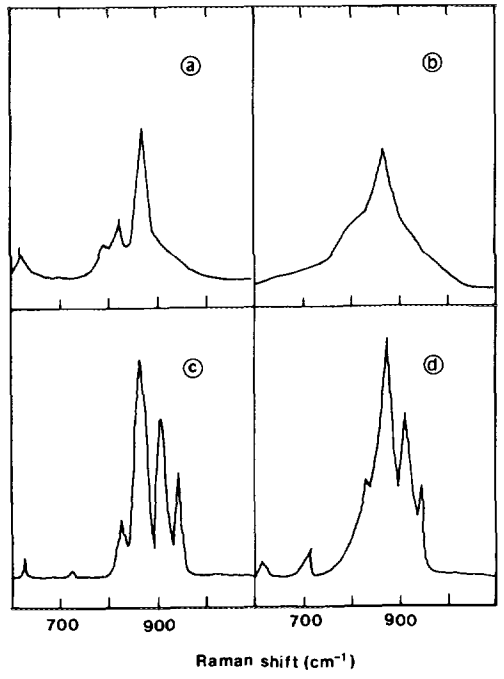

FIG. 6. Raman spectra of differents V–Mg–O samples: (a) 7VO/MgX, (b) 18VO/MgO-2, (c) 48VO/MgX, and (d) 38V/MgO-2.

B.E.'s corresponding to the O1s and Mg2p lines were obtained. With respect to the O1s line, except in the 19V/MgO-1 sample in which two bands at 530.1 and 531.2 eV were obtained, in the other samples only one band was observed.

The intensities of the signals corresponding to the V2$p_{3/2}$ and Mg2p were measured and atomic ratios on the catalyst surface, $(V/Mg)_{XPS}$, were calculated (Table 3). The relationship $(V/Mg)_{XPS}$ and the V/Mg atomic ratios obtained by chemical analysis, $(V/Mg)_{CA}$, are presented in Fig. 7. For the VO/MgX series similar values for the V/Mg ratio at surface and bulk can be observed, although on catalysts with a high vanadium content a V-enrichment of the surface was found.

On MgO-impregnated samples with low vanadium content, lower $(V/Mg)_{XPS}$ ratios with respect to the VO/MgX series were obtained. When the V content is high, a V-enrichment of the catalyst surface has been observed.

Catalytic Results

The catalytic properties of V–Mg–O during the oxidative dehydrogenation of propane are presented in Table 4. Depending on the vanadium content and/or on the catalyst preparation procedure, differences in total activity as well as in selectivity to propene were obtained. Partially oxygenated products were not observed on any catalysts.

From a comparative point of view, the influence of the reaction temperature on the propane conversion, obtained at the same reaction conditions on different V–Mg–O catalysts, is shown in Fig. 8. The highest activity is obtained for the 20V/MgX catalyst.

TABLE 3

XPS Results of V–Mg–O Catalysts

Sample	Binding energy (eV)				$(V/Mg)_{XPS}$ atomic ratio
	C1s	O1s	V2$p_{3/2}$	Mg2p	
7VO/MgX	284.9; 289.4	530.0	517.1	48.9	0.0218
20VO/MgX	284.9; 289.4	530.3	517.2	48.9	0.1048
34VO/MgX	284.9; 289.7	530.3	517.2	49.3	0.2179
48VO/MgX	284.9; 288.9	530.0	517.2	49.5	0.5384
18VO/MgO-2	284.9; 289.3	530.4	517.3	49.2	0.0351
38VO/MgO-2	284.9; 289.7	530.2	517.3	49.5	0.4520
19V/MgO-1	284.9; 289.7	530.1; 531.2	517.1	49.3	0.0545
19V/MgO-3	284.9; 289.7	530.6	517.3	49.5	0.0548

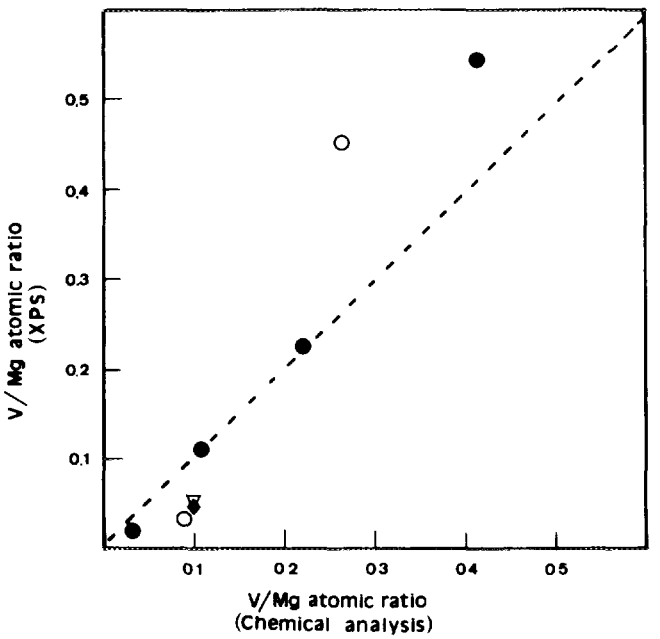

FIG. 7. V/Mg XPS atomic ratio vs V/Mg chemical atomic ratio: VO/Mg*X* series (●), VO/MgO-2 series (○), 19V/MgO-1 sample (▽), and 19V/MgO-3 sample (◆).

TABLE 4

Oxidative Dehydrogenation of Propane on V–Mg–O Catalysts[a]

Sample	W/F[b]	X_T (%)	Selectivity C_3H_6 (%)	CO/CO_2 ratio	T (°C)
7VO/Mg*X*	8.9	5.84	40.4	0.53	500
		16.1	35.0	0.59	550
20VO/Mg*X*	2.7	5.37	61.4	0	500
		16.3	43.3	0.36	550
34VO/Mg*X*	8.9	8.41	58.2	0.42	500
		26.1	42.3	0.51	550
48VO/Mg*X*	13.4	6.33	51.6	0.37	500
		16.2	40.1	0.49	550
18VO/MgO-2	8.9	8.32	59.6	0.17	500
		25.4	38.9	0.48	550
38VO/MgO-2	8.9	8.36	50.9	0.40	500
		23.2	33.4	0.59	550
19V/MgO-1	8.9	13.1	44.1	0.47	500
		29.5	27.5	0.57	550
19V/MgO-3	12.4	6.45	63.7	0	500
		16.7	56.4	0.38	550

[a] C_3H_8/O_2/He molar ratio of 4/8/88.
[b] Contact time, W/F, in g_{cat} h (mol C_3H_8)$^{-1}$.

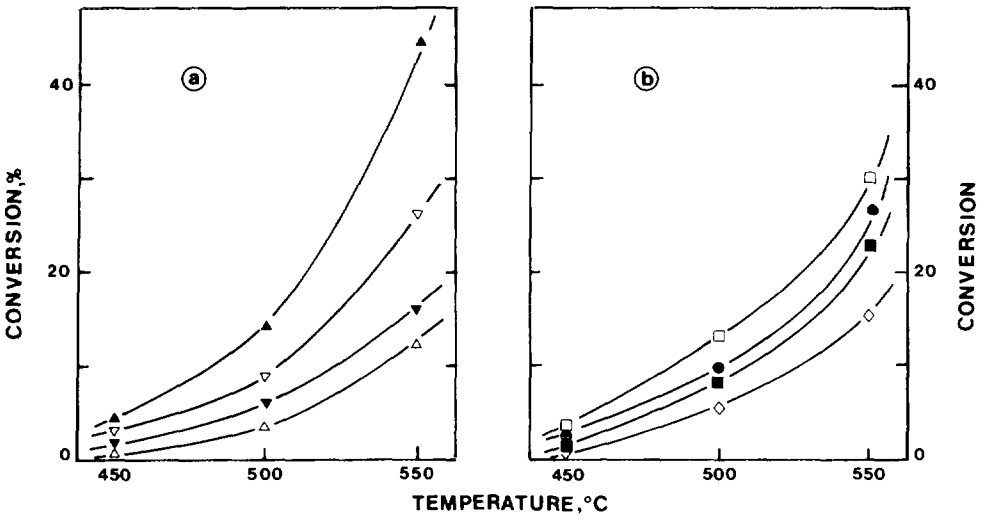

FIG. 8. Influence of reaction temperature on the propane conversion, obtained on the VO/MgX series (a) and on the MgO-impregnated catalysts (b). Symbols 7VO/MgX (△), 20VO/MgX (▲), 34VO/MgX (▽), 48VO/MgX (▼), 18VO/MgO-2 (●), 38VO/MgO-2 (■), 19V/MgO-3 (◇), and 19V/MgO-1 (□). Experimental conditions: C_3H_3/O_2/He molar ratio of 4/8/88; W/F = 12.4 g_{cat} h $(mol_{C_3H_8})^{-1}$.

In Fig. 9 the influence of the contact time on the propane conversion at different reaction temperatures can be seen for the 20V/MgX catalyst. A linear correlation between contact time and propane conversion is observed until 30% of propane conversion.

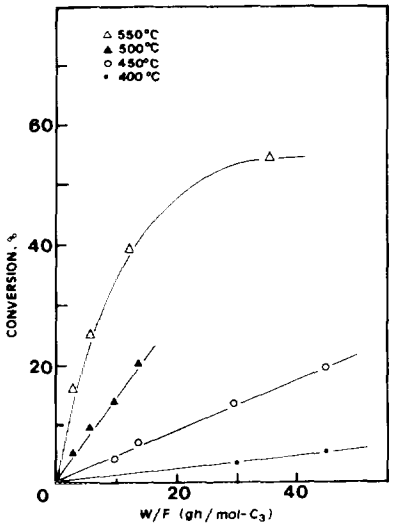

FIG. 9. Influence of the contact time (W/F, in g_{cat} h/mol C_3) on the propane conversion, obtained on the 20VO/MgX catalyst, at different reaction temperatures.

Since sensible differences in the surface areas of the catalysts were obtained, the comparison of the catalytic activity has been carried out from the initial rates of propane conversion (in mol h^{-1} m^{-2}). The influence of the vanadium content on the initial rate for propane conversion is given in Fig. 10. From these data it can be concluded that the maximum activity is also obtained on the 20VO/MgX catalyst. However, on catalysts with the same vanadium content, the activity is different for catalysts prepared using different procedures.

In Fig. 11 it is presented the influence of the propane conversion on the selectivity to propene, at 550°C, on different V–Mg–O catalysts. In the VO/MgX series, the 34VO/MgX sample (Fig. 11a) is the most selective, while in the MgO-impregnated series the 19V/MgO-3 sample (Fig. 11b) is the most selective one. We must indicate that in the temperature range 500–550°C, an influence of the reaction temperature on the selectivity to propene was not observed.

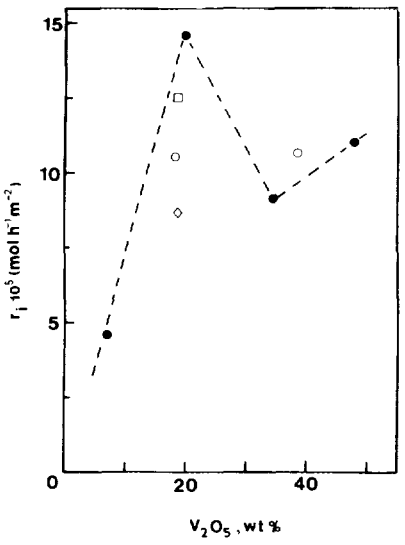

FIG. 10. Influence of the catalyst vanadium content (wt% of V_2O_5) on the initial rate of the propane conversion, obtained at 500°C. Symbols: (●) VO/Mg*X* series, (○) VO/MgO-2 series, (□) 19V/MgO-1 sample, and (◇) 19V/MgO-3 sample.

DISCUSSION

In our calcination conditions, the vanadium content of the catalyst determines the formation of different Mg-vanadates. Thus, on catalysts with vanadium contents greater than 30 wt% the presence of $Mg_3V_2O_8$, α-$Mg_2V_2O_7$, and MgO was observed. On the other hand, on catalysts with vanadium contents $\leq$20 wt% only $Mg_3V_2O_8$ and MgO were detected. This has been consistently found by the different techniques used here, i.e., DRX, IR, and Raman spectroscopies. The only exception was in 7VO/Mg*X* and 18VO/MgO-2 in which $Mg_3V_2O_8$ was detected by IR and Raman spectroscopies but not by XRD. This would indicate that on these samples the crystallites of $Mg_3V_2O_8$ must be smaller than 30 Å.

It has been observed that during impregnation of MgO with an aqueous vanadyl oxalate solution, Mg-oxalate and/or magnesium hydroxide are formed, while during the impregnation of MgO with an aqueous ammonium metavanadate solution, magnesium

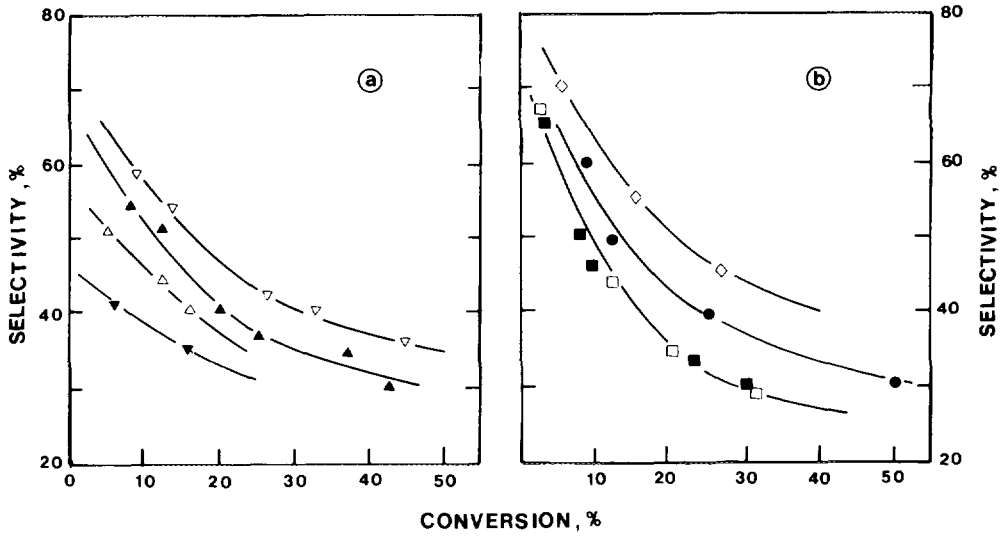

FIG. 11. Influence of the propane conversion on the selectivity to propene obtained, at 550°C, on the VO/Mg*X* series (a) and on the MgO-impregnated catalysts (b). Symbols: 7VO/Mg*X* (△), 20VO/Mg*X* (▲), 34VO/Mg*X* (▽), 48VO/Mg*X* (▼), 18VO/MgO-2 (●), 38VO/MgO-2 (■), 19V/MgO-3 (◇), and 19V/MgO-1 (□).

hydroxide is formed (*23*). This agrees with the DTA results that show the transformation of $Mg(OH)_2$ to MgO (peak at 400°C) for the 19V/MgO-1 sample (Fig. 1e) and the degradation of magnesium oxalate to MgO (peak a ~490°C) in the 18VO/MgO-2 and 38VO/MgO2 samples (Figs. 1f and 1g, respectively).

Large differences in the surface V/Mg atomic ratios depending on the preparation methods were observed (Table 3). Thus, while in VO/Mg*X* series a linear correlation between $(V/Mg)_{XPS}$ and $(V/Mg)_{C.A.}$ atomic ratios occurs, in MgO-impregnated samples a greater influence of the vanadium content on the V/Mg surface atomic ratio can be observed. We propose than these differences are due to the modification of the MgO support during the impregnation step, while in the VO/Mg*X* series these modifications are not observed and a highly homogeneous dispersion of vanadium along the catalysts is obtained.

According to the XPS results, it is more convenient to compare the catalytic properties of V–Mg–O catalysts on the bases of the V/Mg atomic ratios on the catalyst surface. In Fig. 12 the influence of the $(V/Mg)_{XPS}$ atomic ratio on the specific activity for propane conversion (Fig. 12a) and on the selectivity to propene (Fig. 12b) are shown.

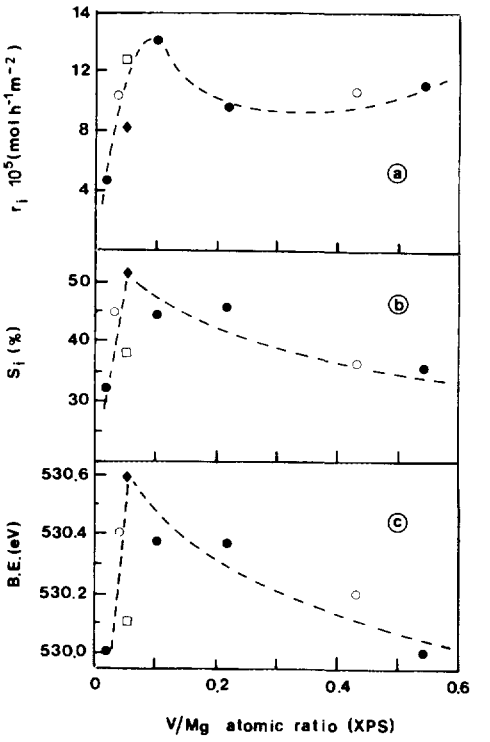

FIG. 12. Influence of the V/Mg surface atomic ratio of the catalysts on: (a) the initial rate for the propane conversion (obtained at 500°C), (b) the selectivity to propene (at a propane conversion level of 20%), and (c) the binding energy of the O1*s* line. Symbols: (●) VO/Mg*X* series, (○) VO/MgO-2 series, (□) 19V/MgO-1 sample, and (◆) 19V/MgO-3 sample.

At low vanadium contents (<25 wt%) only $Mg_3V_2O_8$ is present and, the fact that low $(V/Mg)_{XPS}$ ratios are obtained should indicate the presence of isolated VO_4 tetrahedra on the catalyst surface. In this case, the activity increases when increasing vanadium content but the selectivity to propene shows a maximum at a V/Mg surface atomic ratio of 0.05–0.06. On the contrary, at high vanadium content (>25 wt%), in which $Mg_3V_2O_8$ and α-$Mg_2V_2O_7$ are detected, a V-enrichment of the catalyst surface is obtained, and the presence of associated vanadium complexes should be expected, and consequently a decrease in activity and selectivity is observed.

Differences in the catalytic behavior of metallic orthovanadates has been correlated with their different redox characteristics (*11, 12*). In this sense, a greater reducibility is observed for V–Mg–O samples, in which $Mg_3V_2O_8$ is the main Mg-vanadate phase, than in the corresponding pure magnesium orthovanadate.

On the other hand, in pure Mg-vanadates the highest selectivity to propene and the highest degree of reduction in the vanadium species has been observed for α-$Mg_2V_2O_7$. The fact that this phase presents the highest level of reduction has been related to the presence of corner-sharing VO_4 tetrahedra (*25*).

In our case, the highest catalytic activity is obtained with catalysts with low (V/Mg) surface atomic ratio. In this case, one can

expect to have isolated VO_4 tetrahedron on the catalyst surface. A similar conclusion has been proposed from the results obtained on sepiolite supported vanadium catalysts (*14*).

In addition to this, we must indicate that the TPR-H_2 data, obtained for the VO-Mg*X* catalysts, show two peaks that could correspond to two different vanadium species (*16*). From the comparison between TPR-H_2 data and the catalytic results it has been concluded that a parallelism between catalytic activity and reducibility occurs. In this way, the isolated VO_4 tetrahedra present a greater reducibility than the corresponding pure Mg-orthovanadate.

For comparative purposes, the influence of the $(V/Mg)_{XPS}$ atomic ratio on the binding energies of O1*s* and Mg2*p* lines are considered (Table 3), since it has been proposed that changes in the acid–base properties, which have a clear impact on the catalytic properties, can be monitored by the variation of the XPS energies (*26*). Indeed, in the case of Mg-based mixed oxides, a parallelism between the shift of the binding energies of O1*s* and Mg2*p* in different compounds (as MgO, $MgSiO_3$, $MgSO_4$, or $MgHPO_4$) and their acid-base properties has been established. Thus, for a given atom a decrease in the binding energy of a cation indicates a decrease of the acid strength and vice versa. However, the fact that no parallelism in the shifts of the binding energies of Mg2*p* and O1*s* lines is observed in our V–Mg–O catalysts could indicate that vanadium influences in a different manner than Mg cations the surface oxygens.

In our case, a similar trend in the selectivity to propene (Fig. 12b) and the binding energy of the O1*s* line (Fig. 12c) with the V/Mg surface atomic ratio has been observed on the different V–Mg–O catalysts, in such a way that the higher the shift of the O1*s* line in a given sample, the higher its selectivity to propene (Fig. 13). This could indicate that the incorporation of small amounts of vanadium on a MgO surface

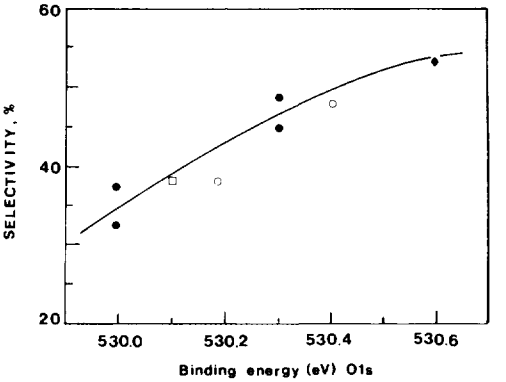

FIG. 13. Selectivity to propene (obtained at 550°C and a propane conversion level of 20%) vs the binding energy of the O1*s* line obtained on different V–Mg–O catalysts. Symbols as Fig. 12.

modifies, not only the redox properties of the system, but also the acid–base character of the oxygens present on the catalyst surface.

However, on catalysts with a very low V/Mg ratios at the catalyst surface, the presence of a greater number of Mg sites can be responsible for the lower selectivity to propene.

It has been proposed that the selectivity of a catalyst during the selective oxidation of alkanes and aromatic hydrocarbons (*27*) and the oxidative dehydrogenation of alkanes (*9*) can be related with the oxidation degree of the surface. Then, it is not doubt that the acid–base character of the catalyst surface oxygens must play an important role for the oxidative dehydrogenation of alkanes, as has been proposed for the selective oxidation of olefins (*28*).

In the other hand, the shift of the O1*s* binding energy in mixed oxide catalysts has been related to the nucleophilicity of the oxygens of the catalyst. The higher the nucleophilicity, the lower the binding energy of the O1*s* and the better the catalytic properties for the selective oxidation of olefins (*29*). In this way, the oxidation of olefins occurs by the formation of C–O bonds.

According to this, and from the data shown in Fig. 13, it can be proposed that in

V–Mg–O catalysts the lower nucleophilicity of the oxygen species, the higher the selectivity to the propane oxydehydrogenation. For this reason, the selectivity to olefins observed for the oxidative dehydrogenation of alkanes could be associated with the presence of VO_4 tetrahedra that limit the possibilities for alkene to be activated through an allylic mechanism and therefore by the formation of C–O bonds. A similar conclusion has been recently proposed (*30*). In addition, the absence of double V=O bonds limits the possible incorporation of oxygen in the intermediate reaction products.

According to the mechanism proposed for the selective oxidative dehydrogenation of alkanes (*4*), the propane is activated by the catalyst that abstract an H atom from the molecule to form an adsorbed propyl radical and a surface OH group. In this case it has been suggested that the oxidation reaction is initiated by highly reactive surface oxygen species. This active oxygen species could be related with the presence of isolated VO_4 tetrahedra (in V–Mg–O samples containing $Mg_3V_2O_8$ as the main Mg-vanadate phase) or with the presence of corner-sharing VO_4 tetrahedra (in samples containing α-$Mg_2V_2O_7$). The formation of tetrahedral V^{5+} species are not limited to the case of V–Mg–O catalysts. Thus, V/SiO_2 (*31, 32*), V-silicalite (*30*), V/Al_2O_3 (*33*), V/Sepiolite (*14*), and VAPO-5 (*34*) catalysts do also present isolated VO_4 tetrahedron, as the main V-species, showing a good selectivity for the oxidative dehydrogenation of alkanes. However, in the last cases, this is possible only at low vanadium contents, while on V–Mg–O catalysts the formation of tetrahedral vanadium species occurs also at higher vanadium contents.

In conclusion, the catalytic properties of V–Mg–O catalysts for the oxidative dehydrogenation of propane depend on the catalyst preparation methods, being the activity and selectivity higher on samples with low V/Mg surface atomic ratios. In this case, isolated VO_4 species are present on the catalyst surface and its higher selectivity could be related with the lower nucleophilic character of the oxygen species on the catalyst surface.

ACKNOWLEDGMENTS

The financial support by Comisión Interministerial de Ciencia y Tecnología (Project MAT 607/91) is gratefully acknowledged. The authors thank Professor J. L. G. Fierro for assisting in the XPS measurements.

REFERENCES

1. Kung, H. H., and Chaar, M. A., U.S. Patent 4,772,319 (1988).
2. Chaar, M. A., Patel, D., and Kung, H. H., *J. Catal.* **109,** 463 (1988).
3. Siew Hew Sam, D., Soenen, V., and Volta, J. C., *J. Catal.* **123,** 417 (1990).
4. Chaar, M. A., Patel, D., Kung, M. C., and Kung, H. H., *J. Catal.* **105,** 483 (1987).
5. Simakov, A. V., Sazonova, N. N., Ven-yaminov, S. A., Belonestnyhk, J. P., Rozhdestvenskaya, N. N., and Isagulyants, G. V., *Kinet. Catal.* **30,** 598 (1987).
6. Simakov, A. V., and Veniaminov, S. A., *React. Kinet. Catal. Lett.* **28,** 67 (1985).
7. Kung, M. C., and Kung, H. H., *J. Catal.* **128,** 287 (1991).
8. Hanuza, J., Jezowska-Trzebiatowska, B., and Oganowski, W., *J. Mol. Catal.* **29,** 109 (1985).
9. Castiglioni, J., Poix, P., and Kieffer, R., *in* "Proceedings, 10th International Congress on Catalysis, Budapest, July 1991," p. 218.
10. Corma, A., López Nieto, J. M., Paredes, N., Pérez, M., Shen, J., Cao, M., and Suib, S. L., *in* "New Developments in Selective Oxidation by Heterogeneous Catalysis" (P. Ruiz and B. Delmon, Eds.), Stud. Surf. Sci. Catal., Vol. 72, p. 213. Elsevier, Amsterdam, 1992.
11. Owen, O. S., Kung, M. C., and Kung, H. H., *Catal. Lett.* **12,** 45 (1992).
12. Patel, D., Andersen, P. J., and Kung, K. K., *J. Catal.* **125,** 132 (1990).
13. Corma, A., López Nieto, J. M., Paredes, N., Pérez, M., and Rajadell, M. J., *in* "Proceedings, XIII Iberoamerican Symposium on Catalysis, Segovia, 1992" Vol. 1, p. 75.
14. Corma, A., López Nieto, J. M., Paredes, N., and Pérez, M., *Appl. Catal.* **97,** 159 (1993).
15. Kung, M. C., and Kung, H. H., *J. Catal.***134,** 668 (1992).
16. Corma, A., López Nieto, J. M., Paredes, N., Dejoz, A., and Vazquez, I., preprint, "II World Congress on New Development in Selective Oxidation, Benalmádena, 1993," in press.
17. Michalakos, P. M., Kung, M. C., Jahan, I., and Kung, H. H., *J. Catal.* **140,** 226 (1993).

18. Clark, G. M., and Morley, R., *J. Solid State Chem.* **16,** 429 (1976).
19. Putanov, P., Kis, E., Boskovic, G., and Lazar, K., *Appl. Catal.* **73,** 17 (1991).
20. Choudhary, V. R., and Pondit, M. Y., *Appl. Catal.* **71,** 265 (1991).
21. Scofield, J. H., *J. Electron Spectrosc. Relat. Phenom.* **8,** 129 (1976).
22. Vullis, M., and Starke, K., *J. Phys. E.* **10,** 158 (1978).
23. Paredes, N., Ph.D. thesis, Universidad Autónoma, Madrid, 1993.
24. Occelli, M. L., and Stencel, J. M., *in* "Fluid Catalytic Cracking Role in Modern Refining" (M. L. Occelli, Eds.), ACS Symp. Ser., Vol. 375, p. 195. ACS, Washington, DC, 1988.
25. Guerrero-Ruiz, A., Rodriguez Ramos, I., Fierro, J. L. G., Soenen, V., Herrman, J. M., and Volta, J. C., *in* "New Development in Selective Oxidation by Heterogeneous Catalysis" (P. Ruiz and B. Delmon, Eds.), Stud. Surf. Sci. Catal., Vol. 72, p. 203. Elsevier, Amsterdam, 1992.
26. Noller, H., Lercher, J. A., and Vinex, H., *Mater. Chem. Phys.* **18,** 577 (1988).
27. Cavani, F., Centi, G., Trifiro, F., and Gasselli, R., *Catal. Today* **3,** 185 (1988).
28. Dadyburjor, D. B., Jewur, S. S., and Ruckenstein, E., *Catal. Rev.-Sci. Eng.* **19,** 293 (1979).
29. Zhdan, P. A., Shepelin, A. P., Osipova, Z. G., and Sokolovskii, V. D., *J. Catal.* **58,** 8 (1979).
30. Bellusi, G., Centi, G., Perathoner, S., and Trifiró, F., *in* "Proceedings, Symposium on Catalytic Selective Oxidation, August 1992," p. 1242. American Chemical Society, Washington DC, 1992.
31. Erdöhelve, A., and Solymosi, F., *J. Catal.* **123,** 31 (1990).
32. Le Bars, J., Vedrine, J. C., Auroux, A., Trautmann, S., and Baerns, M., *Appl. Catal.* **88,** 179 (1992).
33. Andersen, P. J., and Kung, H. H., *in* "Proceedings, 10th International Congress on Catalysis, Budapest, July 1992," p. 12.
34. Concepción, P., López Nieto, J. M., and Pérez-Pariente, *Catal. Lett.*, **19,** 333 (1993).